Available online at www.sciencedirect.com
ScienceDirect
ELSEVIER
Journal of the European Ceramic Society 26 (2006) 2867–2875
ECERS
www.elsevier.com/locate/jeurceramsoc

Broad-band dielectric response of $PbMg_{1/3}Nb_{2/3}O_3$ relaxor ferroelectrics: Single crystals, ceramics and thin films

V. Bovtun [a,*], S. Veljko [a], S. Kamba [a], J. Petzelt [a], S. Vakhrushev [b], Y. Yakymenko [c], K. Brinkman [d], N. Setter [d]

[a] *Institute of Physics, ASCR, Na Slovance 2, 182 21 Prague 8, Czech Republic*
[b] *A. F. Ioffe Physical Technical Institute, 194021 St. Petersburg, Russia*
[c] *NTUU "Kiev Polytechnic Institute", Prospect Peremohy 37, 03056 Kyiv, Ukraine*
[d] *Ceramics Laboratory, Swiss Federal Institute of Technology, 1015 EPFL Lausanne, Switzerland*

Available online 10 March 2006

Abstract

Data of the extensive study of dielectric response of relaxor $PbMg_{1/3}Nb_{2/3}O_3$ (PMN) single crystals, ceramics (standard and textured) and thin films (thickness 500 nm, sapphire substrate) in the broad frequency range (3×10^{-3} to 10^{14} Hz) were combined, summarized and analyzed. Influence of the mesoscopic structure, possible strain and defects in ceramics and thin film on both relaxational and phonon dynamics is discussed. The phonon response of PMN single crystal and thin film appears to be very similar, including the soft mode behaviour. Similar to PMN crystals, the dielectric response of PMN ceramics and films is mainly determined by relaxational dynamics of polar nanoclusters. Flipping and breathing of the clusters are assumed to be the dominant mechanisms, which can be resolved in the frequency spectra of the complex permittivity. The mesoscopic structure and defects in the ceramics do not result in any significant contribution to additional mechanisms, but influence the dynamics of nanoclusters and lead to pinning of the flipping contribution. In thin films the dielectric response due to cluster dynamics is much more reduced.

Keywords: Dielectric properties; Spectroscopy; Relaxor ferroelectrics; Grain boundaries; Films

1. Introduction and samples

The dielectric properties of the model relaxor ferroelectric lead magnesium niobate $PbMg_{1/3}Nb_{2/3}O_3$ (PMN) were widely investigated during last 45 years, mainly in the low-frequency range,[1,2] but also at high frequencies and microwaves.[1,3–7] Our recent studies of the THz and infrared (IR) dielectric response of PMN single crystals[6] and thin films[8] proves that both lattice vibrations and relaxational dynamics play a fundamental role. The dynamics of polar nanoclusters, related to the structural disorder, is considered to be responsible for the relaxor behaviour and determines the dielectric response of PMN crystals.[6,9,10] In the case of ceramics and thin films, the mesoscopic structure and imperfections (grain boundaries, presence of amorphous or another second phase, etc.) or influence of the substrate and surface layers should be taken into account in addition to the structural (compositional) disorder, characteristic for the crystals. The factors mentioned above can, in principle, provide additional contributions to the dielectric response and influence the dynamics of both polar nanoclusters and crystal lattice, modifying the contributions characteristic for the single crystals. This motivated us to combine the results of our extensive study of the dielectric response of PMN single crystals,[4,6,11] ceramics[7] and thin films[8] for comprehensive analysis.

The difference in the geometry of bulk and thin film samples results in different experimental methods used and consequently in extension of the temperature and frequency ranges of investigation. The variety of experimental methods used, including infra-low-frequency,[11] low- and high-frequency[6] dielectric spectroscopy, microwave measurements,[4] time-domain THz spectroscopy[6,8] and IR reflectivity[6] and transmission[8] spectroscopy, allow us to cover almost the full frequency range (3×10^{-3} to 10^{14} Hz) and study both relaxational and phonon dynamics and their temperature evolution from 10 K to 900 K, i.e. below and above the Burns temperature, including the nonergodic frozen phase. In this paper we discuss results, obtained on the following PMN samples prepared by different processing technologies:

* Corresponding author. Tel.: +420 2 6605 2618; fax: +420 2 8689 0527.
E-mail address: bovtun@fzu.cz (V. Bovtun).

0955-2219/$ – see front matter © 2006 Elsevier Ltd. All rights reserved.
doi:10.1016/j.jeurceramsoc.2006.02.003

(a) Single crystals. For details of sample preparation see refs.[4,6,11]

(b) Standard and textured ceramics.[7] Standard ceramic was hot-pressed at 900 °C and then sintered at 1200 °C. The textured ceramic was made up of thick-film layers. The 100 μm thick films were prepared by rolling a mixture of fine PbO and $MgNb_2O_6$ powders at 200 °C and then stacking them into multilayer bulk samples with a thickness of about 7 mm. The bulk textured sample was hot-pressed at 900 °C and then sintered at 1200 °C. Both standard and textured ceramics contain a small quantity of a second non-perovskite phase (probably pyrochlore phase); nevertheless, they satisfy the goal of our study, to assess the influence of the mesoscopic structure, additional imperfections and inhomogeneities on the dielectric response. Three kind of ceramic samples were investigated. Ceramic 1 and Ceramic 2 samples were prepared from the textured PMN ceramics providing the direction of the measuring electric field along and across the film layers, respectively. Ceramic 3 was prepared from the standard PMN ceramics.

(c) Thin film prepared by chemical solution deposition on sapphire substrate.[8] The 500 nm thick film was polycrystalline with a predominately (1 1 1) out-of-plane orientation and a grain-size of 60 nm.

2. Relaxor behaviour of PMN crystals, ceramics and thin films

The dielectric response of all investigated ceramic samples are similar to that of PMN crystals[6,7] and show a typical relaxor behaviour (see Figs. 1 and 2). Diffuse peaks of the real and imaginary parts of the complex dielectric permittivity $\varepsilon'(T)$ and $\varepsilon''(T)$ move towards higher temperatures on increasing frequency. Dielectric dispersion takes place in a broad temperature region both below and above the temperature of permittivity maximum T_m. Relaxor behaviour was observed also in the low-frequency in-plane dielectric response of the PMN thin film,[8] as well as in the out-of-plane or parallel plate capacitor configurations.[12] A comparison of dielectric data obtained for single crystal, ceramics and thin film (Fig. 3) shows only quantitative, not qualitative differences. The main difference is in absolute values of dielectric parameters. The relative permittivity value at 1 MHz in the maximum at T_m is ~11,000 for crystals, ~8000 for ceramics ~2000 for the film. The same is valid for the dielectric loss: highest loss was observed in crystals, lowest loss in the thin film. The difference between standard and textured ceramics remains within 25%. The $\varepsilon'(T)$ maximum is more diffuse in the thin film than in single crystals. The lowest T_m is in PMN crystals, the highest one in the thin film. The difference in T_m between the film and crystal is about 50 K.

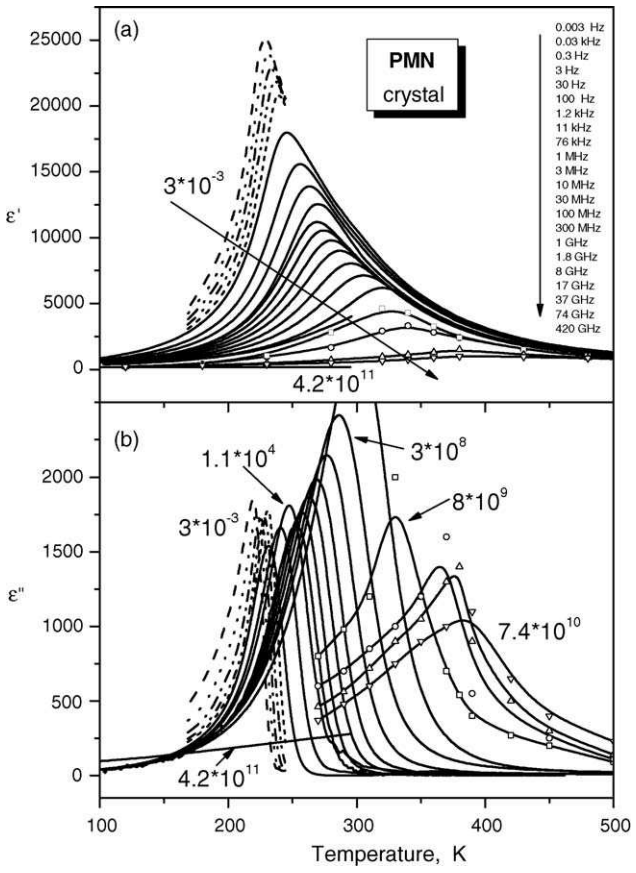

Fig. 1. Temperature dependences of dielectric permittivity ε' and loss ε'' of PMN single crystal at various frequencies. The numbers near curves denote the frequency in Hz.

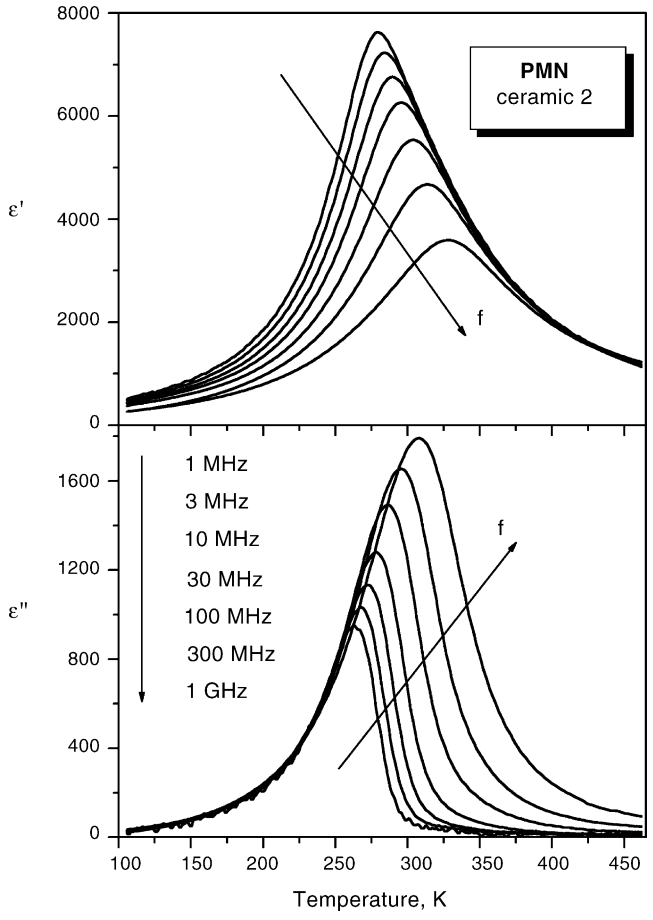

Fig. 2. Temperature dependences of dielectric permittivity ε' and loss ε'' of the textured PMN ceramic (Ceramic 2 sample) at various frequencies.

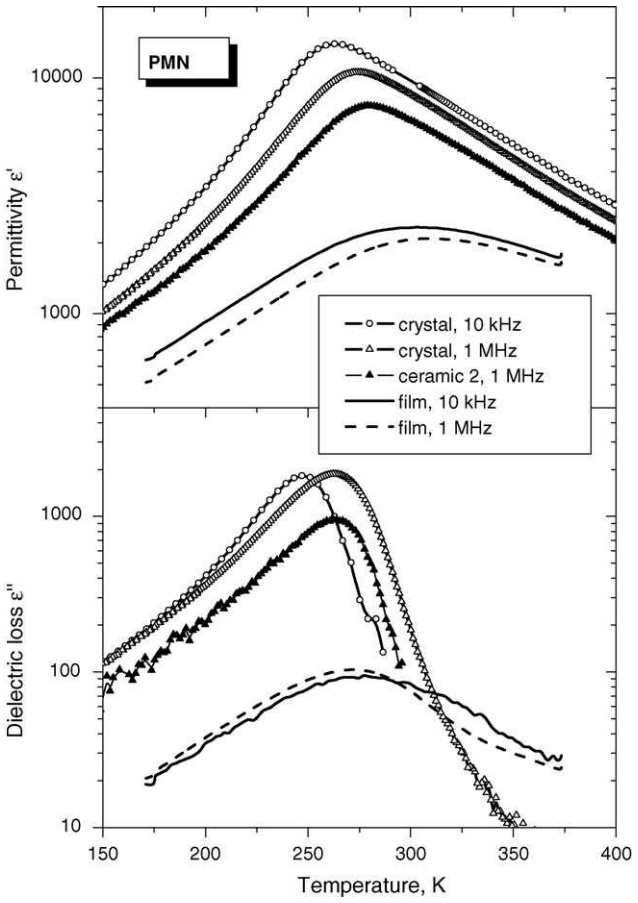

Fig. 3. Temperature dependences of dielectric permittivity ε' and loss ε'' of PMN single crystal, ceramic and thin film.

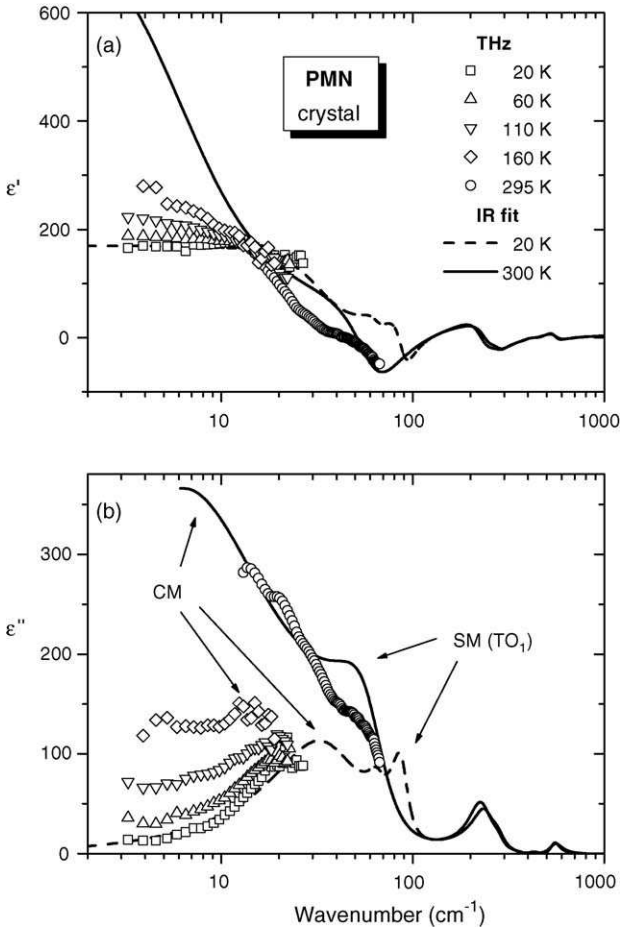

Fig. 4. Frequency dependences of dielectric permittivity ε' (a) and loss ε'' (b) of PMN single crystal in the THz and IR range. Symbols correspond to the THz data, lines—to the fits of IR reflectivity and THz data. SM and CM denote loss peaks corresponding to the soft and central mode, respectively.

The nearly temperature independent (below 300 K) value $\varepsilon' = 175$, revealed in the PMN crystal at 420 GHz, proves that the phonon contribution is much lower than the low-frequency permittivity in all the samples. That is why the observed difference in low- and high-frequency dielectric response between PMN crystal, ceramics and thin film could be mainly attributed to the different strength of the dielectric relaxation which takes place below phonon frequencies. Namely, the highest strength corresponds to PMN crystal, the lowest strength to the film.

3. Soft and central modes in PMN crystals and thin films

IR reflectivity spectra of PMN crystals[6] reveal three main transverse optical modes typical for the simple cubic perovskite structure (Fig. 4). The lowest polar mode (TO_1) displays pronounced temperature dependence and plays the role of the soft mode (SM) in normal ferroelectric perovskites. It partially softens towards the Burns temperature T_d on heating, from $\sim$87 cm^{-1} at 20 K to 54 cm^{-1} at 300 K according to the Cochran law:

$$v_{SM}^2 = A(T_d - T), \quad (1)$$

where $T_d = 550$–620 K is the extrapolated critical temperature,[6] and v_{SM} the SM frequency. No phonon anomaly was observed near the temperature of low-frequency permittivity maximum $T_m \sim 265$ K. The phonon contribution to permittivity increases from $\sim$40 at 20 K to $\sim$100 at 300 K and does not account for the whole permittivity. The TO_1 soft mode is underdamped and well resolved in THz and IR spectra at 10–300 K. Another excitation was observed below the SM frequency (Fig. 4) and called central mode (CM). It consists of two components. The first, fast component appears near 30 cm^{-1} ($\sim$1 THz) for all temperatures below room temperature and contributes about 130 to the static permittivity at 20 K.[6] The second, slow component is observed as a high-frequency wing of the dielectric relaxation which sets mainly below the far-IR range, below room temperature, and slows down and broadens on cooling.

Translucency of the PMN thin film in the far-IR range allowed us to study its IR transmission spectra in a wide temperature interval 10–900 K.[8] Dielectric loss spectra calculated from the fit of the transmission spectra of PMN films are shown in Fig. 5. The observed loss maxima indicate the presence of two excitations below 100 cm^{-1} which were attributed to the soft and central mode.[8] Their temperature dependences are shown in Fig. 6. Soft TO_1 mode slightly softens from 60 cm^{-1} (900 K) on cooling, but below 450 K it starts to harden and follows the Cochran law (1) with the extrapolated critical temperature

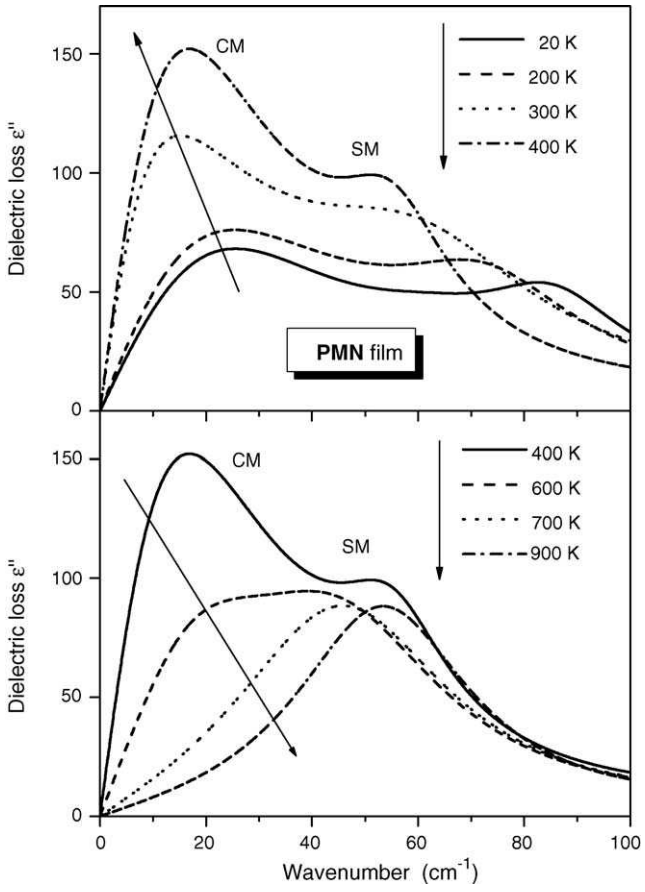

Fig. 5. Dielectric loss spectra of PMN thin film calculated from the fit of IR transmission spectra at various temperatures.

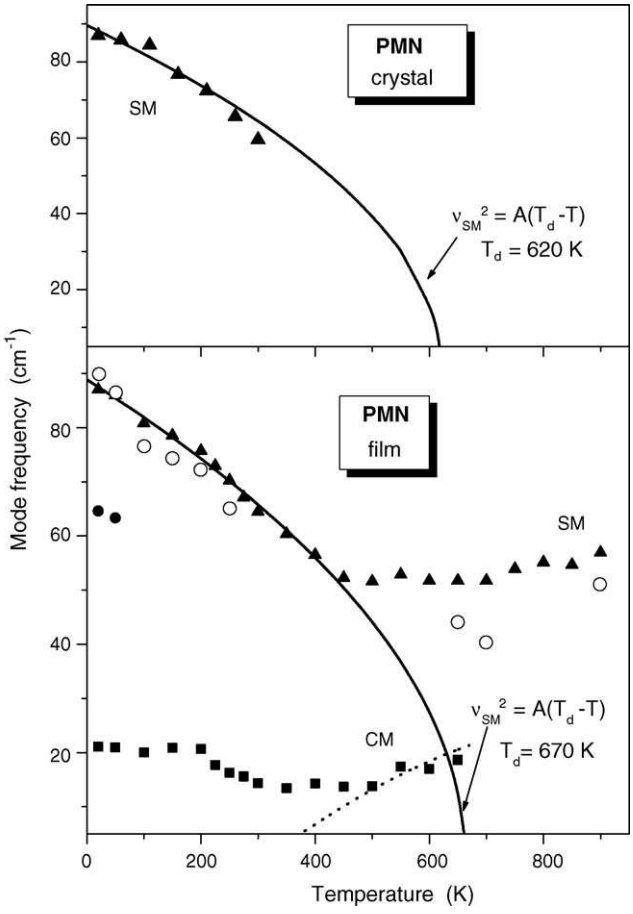

Fig. 6. Temperature dependences of the soft mode (SM) and central mode (CM) frequencies in PMN crystal and thin film. Solid and open symbols mark data obtained from IR spectra (crystal and film) and inelastic neutron scattering spectra (crystal), respectively. CM is overdamped, therefore the frequency of loss maximum corresponding to ν_{CM}^2/γ_{CM} is plotted. The Cochran fit of the SM is shown by the solid line, the slowing down of the CM is schematically shown by the dashed line.

$T_d = (670 \pm 10)$ K and $A = (11.9 \pm 0.2)$ K^{-1}. The critical temperatures, estimated for both single crystal and thin film, are close to the Burns temperature reported for PMN single crystals.[1,2,13] The damping of the SM is only slightly temperature dependent. It increases from 34 cm^{-1} (at 20 K) to 50 cm^{-1} (at 300 K) and at higher temperatures it remains temperature independent within the accuracy of our fits. These results show that the SM is underdamped in IR spectra in the whole investigated temperature range, unlike the inelastic neutron scattering spectra where the so called "waterfall" was observed between the freezing and Burns temperatures due to the apparent overdamping of SM.[8,14,15]

The SM frequency and its temperature dependence in the thin PMN film agree well (Fig. 6) with that in the PMN crystal determined from the IR reflectivity[6] below 300 K and inelastic neutron scattering spectroscopy[14] at low temperatures and above T_d. It is seen that the lattice vibrations are not appreciably influenced by the possible strain, microstructure and defects in the film, and that the lattice response of relaxors in thin films does not differ appreciably from that in single crystals. The situation differs from the situation in incipient ferroelectrics[16] where the soft mode in films, which represents the substantial contribution to the static permittivity, is strongly influenced by strains and microstructure. On the other hand, in relaxors the main contribution to permittivity stems from the polar cluster dynamics below the phonon frequencies.[6,9,10]

The central mode in the PMN thin film was revealed below the Burns temperature $T_d = 670$ K as a new overdamped excitation which appears below the SM frequency and results in appreciable decrease in the IR transmission below 40 cm^{-1}. Similar to the PMN crystal, the CM consists of two components which split below ~500 K. The frequency of the slow component rapidly decreases on cooling and shifts out of the far-IR range below 400 K (see dash line in Fig. 6). We believe that this CM component corresponds to the microwave and high-frequency relaxation[3,4,6,8] observed in PMN crystal below 500 K (Fig. 7). Yet another broad excitation (fast CM component) remains at the low-frequency end of the IR spectra down to 20 K. Its loss maximum lies near $\nu_{CM}^2/\gamma_{CM} = 20$ cm^{-1} (ν_{CM} and γ_{CM} are the CM frequency and damping), see Fig. 6. Taking into account the high damping of the central mode in the thin film,[8] this value corresponds well to the ν_{CM} ~30 cm^{-1}, estimated for the single crystal.[6] So, like the soft mode, the fast component of the central mode behaves similarly in both single crystal and thin film. It splits from the soft mode response below the Burns temperature and was previously assigned to activated short-wavelength phonons due to the breaking of

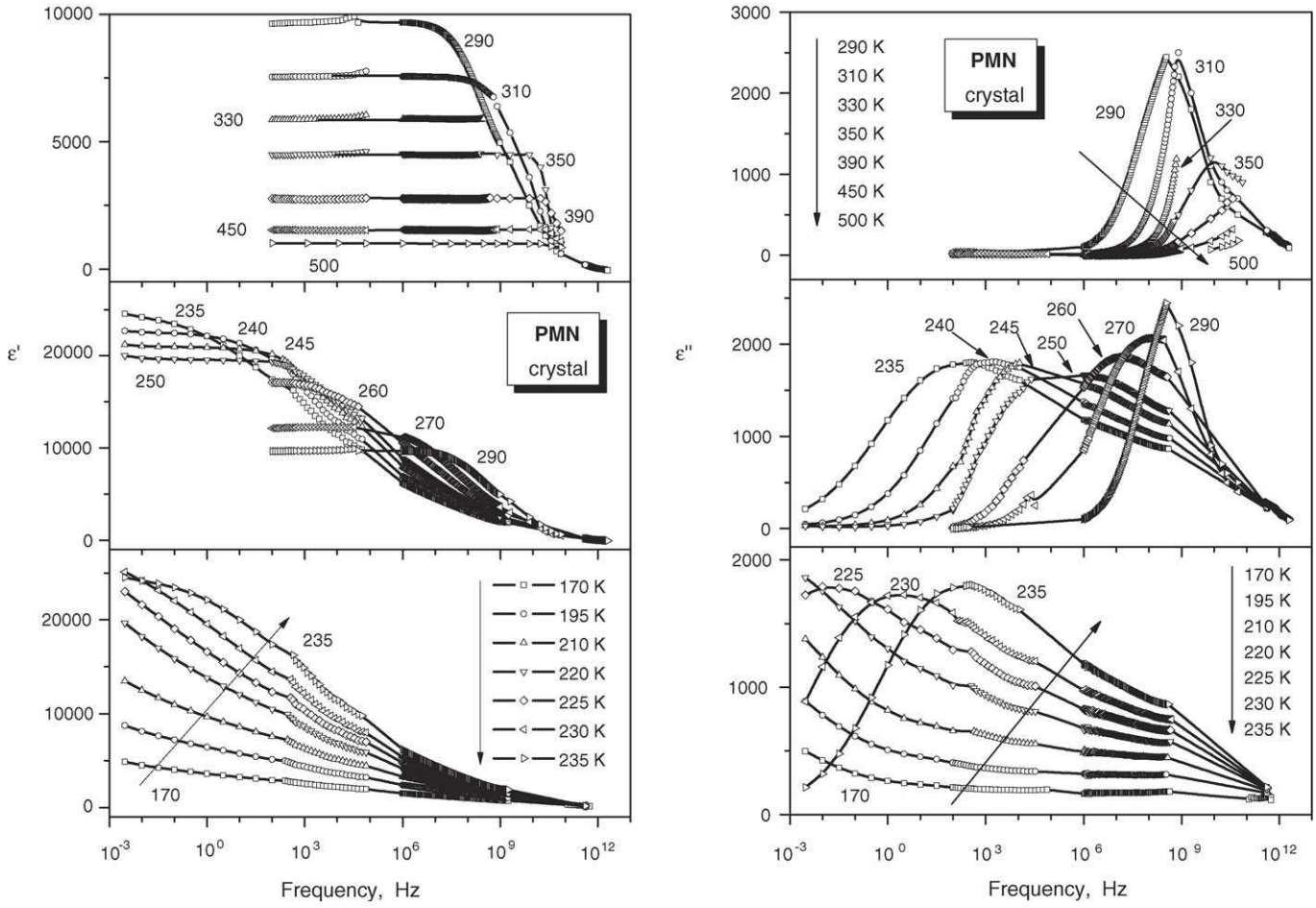

Fig. 7. (a) Frequency dependences of dielectric permittivity ε' of PMN single crystals at various temperatures. The numbers near curves denote the temperature in K. (b) Frequency dependences of dielectric loss ε'' of PMN single crystals at various temperatures. The numbers near curves denote the temperature in K.

local symmetry as a consequence of polar nano-clusters.[6,8] According to our most recent explanation,[15] the SM is triply degenerate above T_d, but in the polar phase or in polar clusters below T_d it should split into the stiffer A_1 component, which hardens according to Cochran law on cooling (corresponds to the TO_1 SM), and the softer E component, which stays at lower frequencies (corresponds to the fast CM component). This component was observed as the underdamped SM in the very recent high-resolution inelastic neutron scattering experiment.[17]

The slow central mode component is the relaxational excitation which also originates from the dynamics of polar nanoclusters in PMN[6–8] and develops in the broad-band dielectric dispersion below 400 K.

4. Relaxational dielectric dispersion

The broad-band dielectric dispersion was studied in most detail in PMN single crystals. Temperature evolution of the complex dielectric response of PMN crystals, shown on Fig. 7a and b, is a sum of several experimental studies.[4,6,11] The procedure of combining the experimental data and their detailed analysis will be presented in another paper. Here we would like to address the main features.

Relaxational dielectric spectra of PMN crystals are diffuse (i.e., are non-Debye ones and characterized by the relaxation time distribution) at all temperatures. The loss maximum $\varepsilon''(f)$ appears in the mHz range at 220 K, passes through low-frequency, high-frequency and microwave ranges on increasing temperature and shifts to THz range above 390 K (Fig. 7b). The shape of the $\varepsilon''(\log f)$ dependences is substantially asymmetric between 230 K and 270 K; the low-frequency part below the $\varepsilon''(\log f)$ maximum is less diffused than the high-frequency part above it. The infra-red frequency data indicate that the relaxational loss maximum is also present below the freezing temperature $T_f \approx 200$ K even if it is shifted below the low-frequency edge of our experiments. Here it seems to be superimposed on the background of frequency-independent loss observed in the range of 100 Hz to 100 GHz (Fig. 7b). The asymmetrical shape of $\varepsilon''(\log f)$ dependences and the loss superposition below T_f indicate the presence of at least two contributions to the observed relaxational dispersion. Both contributions are diffuse and overlapped, and therefore not well separated in the dielectric spectra. The presence of two relaxational contributions (and consequently, two polarization mechanisms) above T_f was evidenced also in the earlier studies.[4,6,9] The first, lower-frequency mechanism is responsible for the observed relaxational $\varepsilon''(f)$ maximum and prevails at high temperatures. The second, higher frequency

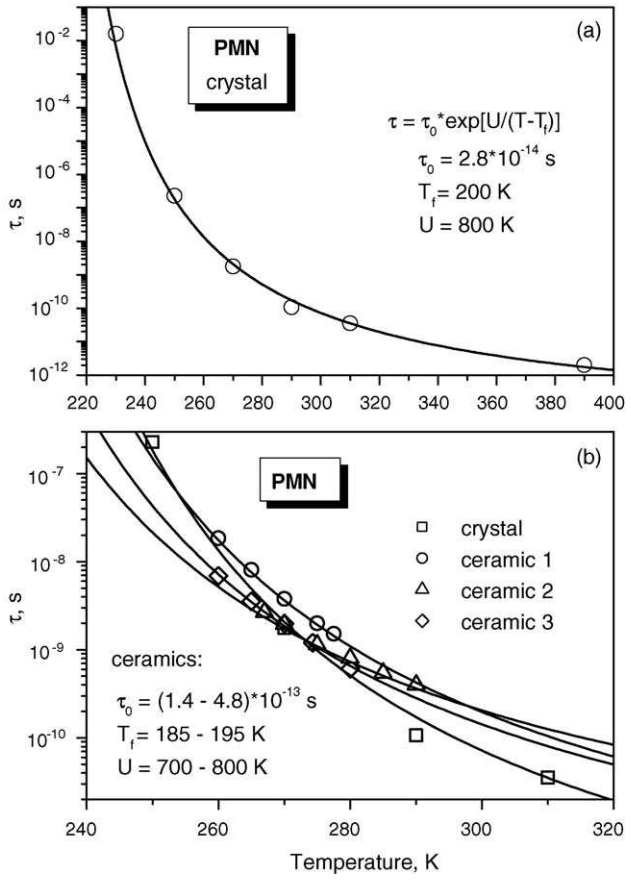

Fig. 8. Temperature variation of the mean relaxation time of the lower-frequency relaxation mechanism in PMN single crystal (a) and ceramics (b). Symbols and solid lines correspond to the experimental data and Vogel–Fulcher fits, respectively.

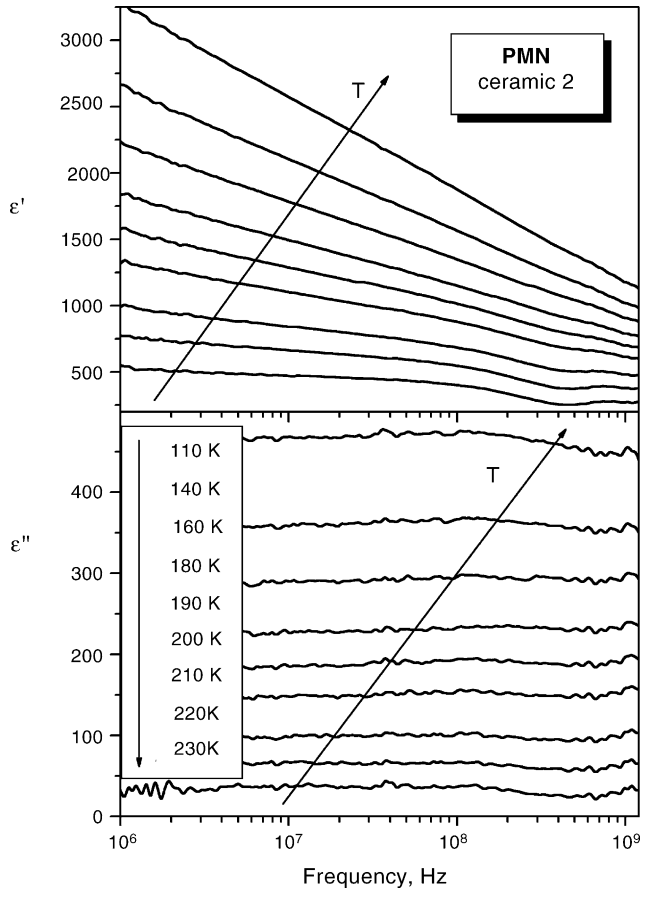

Fig. 9. Frequency dependences of dielectric permittivity ε' and loss ε'' of the textured PMN ceramic (Ceramic 2 sample) at low temperatures.

mechanism is responsible for the frequency-independent loss observed at low temperatures. The mean relaxation time of the first mechanism follows the Vogel–Fulcher law

$$\tau(T) = \tau_0 \exp\left(\frac{U}{T - T_f}\right), \quad (2)$$

with the freezing temperature $T_f \approx 200$ K and activation energy $U \approx 800$ K above 230 K (Fig. 8a). As the infra-red-frequency data the loss maximum is observed even below T_f, the freezing of this relaxation is only partial and deviations from the Vogel–Fulcher law should take place below 230 K.

Similar to the PMN crystals, the presence of two contributions to the relaxational dielectric dispersion was observed also in PMN ceramics.[7] Below 230 K the frequency-independent loss spectra $\varepsilon''(f)$ are revealed (Fig. 9). On increasing temperature, a maximum of $\varepsilon''(f)$ appears above 250 K (Fig. 10), passes through the high-frequency range and shifts to microwave range above 330 K. The permittivity-dispersion range shifts correspondingly to higher frequencies and above 330 K the dielectric dispersion sets-in in the microwave range. Like in the crystals, relaxational dielectric dispersion in PMN ceramics is of non-Debye type and is characterized by a wide distribution of relaxation times. The distribution is very wide below 230 K (where frequency-independent loss spectra are observed), becoming

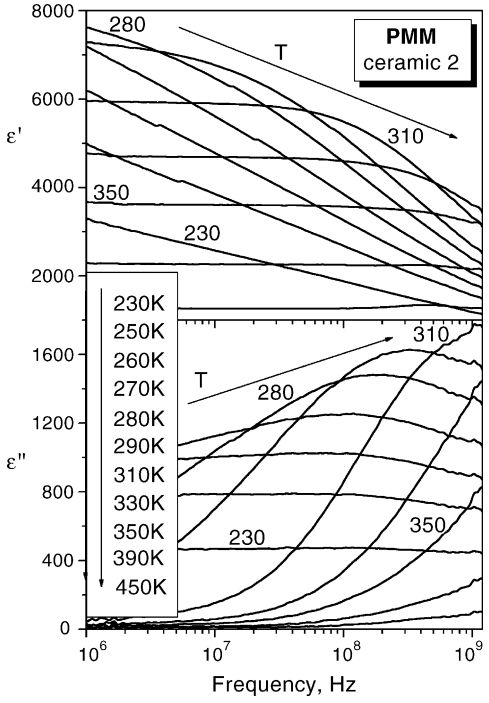

Fig. 10. Frequency dependences of dielectric permittivity ε' and loss ε'' of the textured PMN ceramic (Ceramic 2 sample) at high temperatures. The numbers near curves denote the temperature in K.

narrower on increasing temperature. The mean relaxation time of the first, lower-frequency relaxation mechanism follows the Vogel–Fulcher law (2) with parameters similar to that in PMN crystals (Fig. 8b).

Relaxational dielectric dispersion in PMN thin films was studied only at low frequencies (Fig. 3), but then the relaxational component of central mode was clearly detected in the far-IR spectra at high temperatures (see Figs. 5 and 6). Therefore, relaxational dynamics in the PMN film seems to be similar to the dynamics in bulk PMN. The relaxational contribution is substantial also in the dielectric response of PMN thin film, even if it is reduced compared with that of PMN crystals and ceramics.

5. General scheme of the dielectric response

The experimental results for PMN crystal, ceramics and film coincide with the general scheme of the dielectric response of relaxor ferroelectrics[9,10] based on the concept of polar nanoclusters. Paraelectric SM, observed above the Burns temperature, tends to soften partially down to T_d, where the local ferroelectric soft mode within polar clusters splits and its component parallel to the local polarization hardens on cooling below T_d. This SM is, however, not dominant in the dielectric response. Dielectric response below T_d is mainly determined by the dynamics of polar nanoclusters, which appear below the Burns temperature and are responsible for the CM split from the SM response. The fast component of the CM, which stays in the THz range down to helium temperatures, corresponds presumably to the softer SM component polarized normal to the local cluster polarization. The slow CM component is related to the relaxational cluster dynamics and rapidly slows down on cooling. The dominant mechanisms of this dynamics are dipole reversal (flipping) of polar clusters and fluctuations of polar-cluster volume (breathing). Presumably, the microwave dispersion close to T_d is due to the cluster dipole flipping. The interactions among polar clusters cause freezing (at least, partial) of the local dipole moments when approaching T_f, essentially suppressing cluster flipping in weak fields below T_m. Consequently, the breathing mechanism contribution to the dielectric response prevails below T_m and is responsible for the frequency-independent dielectric loss at low temperatures.

According to a phenomenological thermodynamic theory of this mechanism,[18,19] the broad distribution of relaxation times stems from structural inhomogeneities (Mg^{2+} and Nb^{5+}) at the perovskite B-sites, which cause random fields and a broad distribution of activation energies for highly anharmonic hopping of Pb atoms. The distribution width should be comparable with the mean barrier height so that some barriers exist essentially down to zero values. These barriers cause the high-frequency losses down to very low temperatures. Taking this barrier distribution independent of temperature, the distribution of relaxation times broadens exponentially on cooling and the low-frequency end of the relaxation-frequency distribution quickly passes beyond the frequency range of our measurements. This results in the constant loss in the achievable frequency range.

In the framework of the general scheme, two observed contributions to the relaxational CM component can be assigned

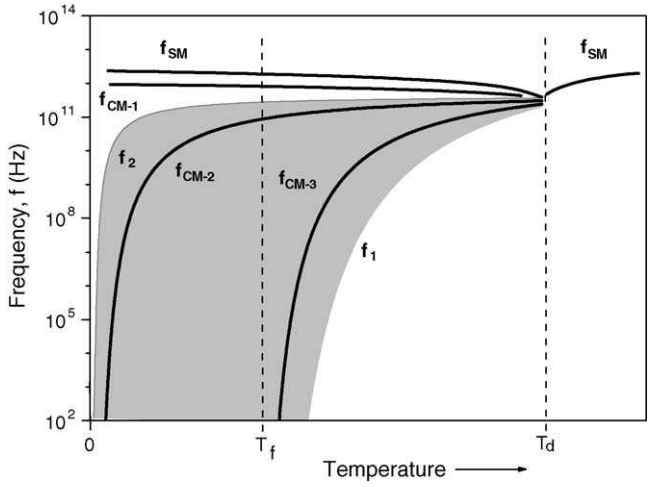

Fig. 11. Scheme of temperature evolution of the soft and central mode frequencies. Curves f_{SM} and f_{CM-1} correspond to the frequencies of the soft mode and fast component of central mode. Curves f_{CM-2} and f_{CM-3} correspond to the mean frequencies of the relaxational components of central mode assigned to the breathing and flipping of polar clusters, respectively. Curves f_1 and f_2 are the lower and upper limits of the relaxation frequencies distribution. The grey filled region denotes the frequency–temperature range of relaxational dynamics of polar clusters.

to the cluster breathing mechanism (low-temperature dispersion characterised by the frequency-independent loss) and to the cluster flipping mechanism (high-temperature relaxation, characterised by the Vogel–Fulcher law). Temperature evolution of SM and CM component frequencies is schematically presented in Fig. 11. Here, the Vogel–Fulcher law is assumed for the mean frequency of flipping mechanism (CM-3 component) while the Arrhenius law is assumed for the mean frequency of breathing mechanism (CM-2 component) which seems to be active down to helium temperatures. Because both components are characterized by a wide distribution of relaxation times or frequencies and are therefore overlapped in frequency domain, the grey filled region corresponds to slow, relaxational component of central mode. Curves f_1 and f_2 are the lower and upper limits of the relaxation frequencies distribution. It can be seen that the distribution becomes extremely wide near and below the freezing temperature. The details of the ultra-low-frequency part of the dielectric response will be discussed elsewhere.

Summarising, the relaxational dielectric response of PMN film, ceramics and single crystals are qualitatively similar and can be explained by the same mechanisms, polar cluster flipping and breathing, but detailed comparison reveals quantitative differences. Some of them were noted above: the difference in T_m, in the maximal values of the permittivity $\varepsilon'_m(T)$ and loss $\varepsilon''_m(T)$. The comparison of the high-frequency dielectric spectra of PMN ceramics and single crystals (Fig. 12) allows us to estimate the influence of the mesoscopic structure on both flipping and breathing mechanisms.[7] Contribution of cluster flipping mechanism seems to be less pronounced in ceramics and the breathing mechanism responsible for the frequency-independent loss prevails below 250 K (Figs. 9 and 10), unlike the PMN crystals where it dominates only below 200 K (see Fig. 7b and ref.[6]). At high temperatures the contributions of the flipping

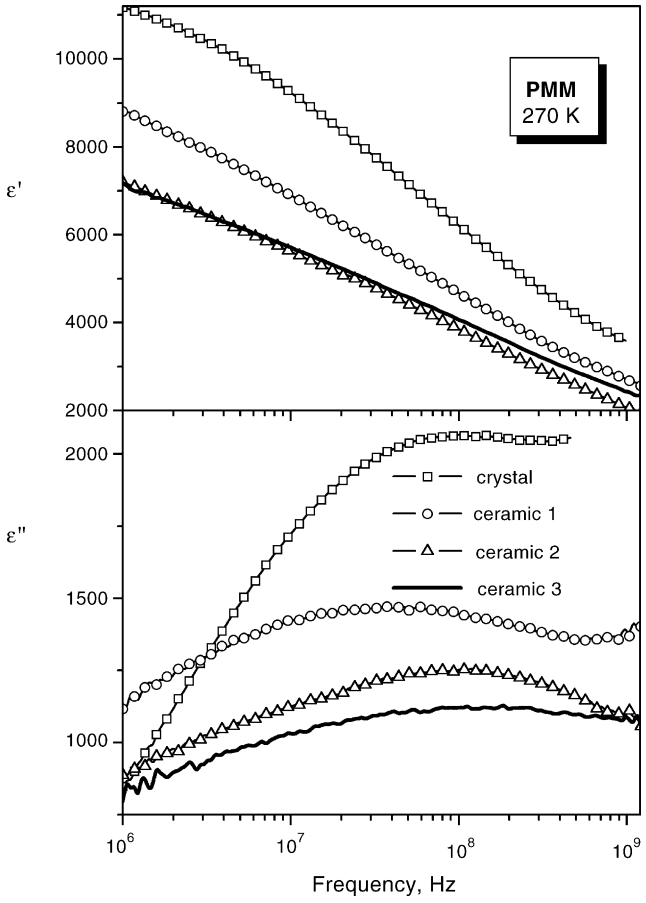

Fig. 12. Frequency dependences of dielectric permittivity ε' and loss ε'' of PMN crystal and ceramics at 270 K.

and breathing mechanisms in PMN ceramics are comparable, in crystals the cluster flipping mechanism seems to dominate. In other words, the mesoscopic structure and imperfections of ceramics influence the dynamics of polar nanoclusters and lead to the weakening of the cluster flipping mechanism contribution, probably, due to the pinning at grain boundaries.

The higher T_m in ceramics and thin film, compared to the T_m in PMN crystal (Fig. 3), can also be explained by the influence of grain boundaries and strain effect of the substrate (in film samples) on the flipping of polar clusters, resulting in more rapid slowing down of its mean frequency on cooling. Consequently, the T_m increases. On the other hand, the freezing temperatures appear to be the same ($T_f \sim 200$ K) in PMN ceramics and crystal (Fig. 8).

6. Conclusions

The phonon response of PMN single crystal and thin film appears to be very similar and is characterized by the same frequency of the underdamped and well resolved SM, which softens only partially towards the Burns temperature on heating, according to the Cochran law, with similar parameters. No phonon anomaly was observed near the temperature of low-frequency permittivity maximum. The fast component of the CM, attributed recently to the SM component perpendicular to local cluster polarization, was observed in far-IR spectra of PMN film and crystal at nearly the same frequency ($\sim$20–30 cm^{-1}) below the Burns temperature. As a result, the phonon contribution to the dielectric permittivity is similar and much lower than the low-frequency permittivity of PMN crystal and films. Possible defects and strain in our thin film have no significant influence on the phonon response of PMN. The same is also valid for the mesoscopic structure of ceramics.

Similar to PMN crystals, the dielectric response of ceramics and films is mainly defined by the slow component of the CM caused by relaxational dynamics of polar nanoclusters. The slow component of CM was observed as a broad-band relaxational dielectric dispersion. Flipping and breathing of polar clusters are considered as dominant mechanisms of the relaxational cluster dynamics. The flipping mechanism is more pronounced in the high-temperature relaxation and essentially freezes when approaching T_f on cooling. The breathing mechanism dominates in the low-temperature relaxation and is responsible for the frequency-independent loss below T_f.

Grain boundaries, the presence of a small amount of the second pyrochlore phase and other possible defects in PMN ceramics do not result in a significant dielectric contribution. Nevertheless, mesoscopic structure and imperfections of ceramics influence the dynamics of polar nanoclusters and lead to the weakening of the cluster flipping mechanism contribution. In thin films, the dielectric response due to the cluster dynamics is strongly reduced.

Acknowledgements

The work was supported by the Grant Agency of the Czech Rep. (project No. 202/04/0993), Czech Acad. Sci. (projects Nos. A1010213 and AVOZ-10100520) and Czech Ministry of Education (project COST No. OC525.20/00).

References

1. Smolenskii, G. A., Bokov, V. A., Isupov, V. A., Krainik, N. N., Pasynkov, R. E. and Sokolov, A. I., *Ferroelectrics and Related Materials*. Gordon & Breach Sci. Publishers, New York, 1984.
2. Samara, G. A., Properties of compositionally disordered ABO_3 perovskites. *J. Phys.: Condens. Matter*, 2003, **15**, R367–R411.
3. Poplavko, Y. M., Bovtoun, V. P., Krainik, N. N. and Smolensky, G. A., Microwave dielectric dispersion in lead magnesium niobate. *Fiz. Tverd. Tela*, 1985, **27**, 3161–3163.
4. Bovtoun, V. P. and Leshchenko, M. A., Two dielectric contributions due to domain/clusters structure in the ferroelectrics with diffused phase transitions. *Ferroelectrics*, 1997, **190**, 185–190.
5. Levstik, A., Kutnjak, Z., Filipič, C. and Pirc, R., Glassy freezing in relaxor ferroelectric lead magnesium niobate. *Phys. Rev. B*, 1998, **57**, 11204–11211.
6. Bovtun, V., Kamba, S., Pashkin, A., Savinov, M., Samoukhina, P., Petzelt, J. *et al.*, Central-peak components and polar soft mode in relaxor PMN crystals. *Ferroelectrics*, 2004, **298**, 23–30.
7. Bovtun, V., Veljko, S., Savinov, M., Pashkin, A., Kamba, S. and Petzelt, J., Comparison of the dielectric response of relaxor $PbMg_{1/3}Nb_{2/3}O_3$ ceramics and single crystals. *Integr. Ferroelectr.*, 2005, **69**, 3–10.
8. Kamba, S., Kempa, M., Bovtun, V., Petzelt, J., Brinkman, K. and Setter, N., Soft and central mode behaviour in $PbMg_{1/3}Nb_{2/3}O_3$ relaxor ferroelectric. *J. Phys.: Condens. Matter*, 2005, **17**, 3965–3974.

9. Bovtun, V., Petzelt, J., Porokhonskyy, V., Kamba, S. and Yakimenko, Y., Structure of the dielectric spectrum of relaxor ferroelectrics. *J. Eur. Ceram. Soc.*, 2001, **21**, 1307–1311.
10. Bovtun, V., Porokhonskyy, V., Savinov, M., Pashkin, A., Zelezny, V. and Petzelt, J., Broad-band dielectric response of doped incipient ferroelectrics. *J. Eur. Ceram. Soc.*, 2004, **24**, 1545–1549.
11. Colla, E. V., Koroleva, E. Y., Okuneva, N. M. and Vakhrushev, S. B., Low-frequency dielectric response of $PbMg_{1/3}Nb_{2/3}O_3$. *J. Phys.: Condens. Matter*, 1992, **4**, 3671–3677.
12. Kighelman, Z., Damjanovic, D. and Setter, N., Electromechanical properties and self-polarization in relaxor $Pb(Mg_{1/3}Nb_{2/3})O_3$ thin films. *J. Appl. Phys.*, 2001, **89**, 1393–1401.
13. Ye, Z.-G., Relaxor ferroelectric complex perovskites: structure, properties and phase transitions. *Key Eng. Mater.*, 1998, **155–156**, 81–122.
14. Wakimoto, S., Stock, C., Ye, Z.-G., Chen, W., Gehring, P. M. and Shirane, G., Mode coupling and polar nanoregions in relaxor ferroelectric $Pb(Mg_{1/3}Nb_{2/3})O_3$. *Phys. Rev. B*, 2002, **66**, 224102.
15. Kamba, S., Kempa, M., Berta, M., Petzelt, J., Brinkman, K. and Setter, N., Dynamics of polar clusters in relaxor ferroelectrics. *J. Phys. IV France*, 2005, **128**, 121–126.
16. Ostapchuk, T., Petzelt, J., Zelezny, V., Pashkin, A., Pokorny, J., Drbohlav, I. *et al.*, Origin of soft-mode stiffening and reduced dielectric response in $SrTiO_3$ thin films. *Phys. Rev. B*, 2002, **66**, 235406.
17. Gvasaliya, S. N., Roessli, B., Cowley, R. A., Huber, P. and Lushnikov, S. G., Quasi-elastic scattering, random fields and phonon-coupling effects in $PbMg_{1/3}Nb_{2/3}O_3$. *J. Phys.: Condens. Matter*, 2005, **17**, 4343–4359.
18. Kamba, S., Bovtun, V., Petzelt, J., Rychetsky, I., Mizaras, R., Brilingas, A. *et al.*, Dielectric dispersion of the relaxor PLZT ceramics in the frequency range 20 Hz–100 THz. *J. Phys.: Condens. Matter*, 2000, **12**, 497–519.
19. Rychetsky, I., Kamba, S., Porokhonskyy, V., Pashkin, A., Savinov, M., Bovtun, V. *et al.*, Frequency-independent dielectric losses (1/f noise) in PLZT relaxors at low temperatures. *J. Phys.: Condens. Matter*, 2003, **15**, 6017–6030.